EUROFUSION WP15ER-PR(15) 14601

E Nilsson et al.

Runaway electrons in non-disruptive scenarios in the Tore Supra tokamak

Preprint of Paper to be submitted for publication in
Nuclear Fusion

This work has been carried out within the framework of the EUROfusion Consortium and has received funding from the Euratom research and training programme 2014-2018 under grant agreement No 633053. The views and opinions expressed herein do not necessarily reflect those of the European Commission.

Runaway electrons in non-disruptive scenarios in the Tore Supra tokamak

E. Nilsson[1], Y. Peysson[1], J. Decker[2], J.F. Artaud[1], T. Aniel[1],
M. Irishkin[1], D. Mazon[1] and F. Saint-Laurent[1]

October 17, 2015

[1]CEA, IRFM, F-13108, Saint-Paul-lez-Durance, France

[2]Ecole Polytechnique Fédérale de Lausanne (EPFL), Centre de Recherches en Physique des Plasmas (CRPP), CH-1015 Lausanne, Switzerland

Abstract

Runaway electrons have been detected in the Tore Supra tokamak in low line-averaged density discharges ($\bar{n}_e < 10^{19}\ m^{-3}$) during the current ramp down in non-disruptive tokamak scenarios. Such well-diagnosed discharges with non-transient plasma parameters are suitable for studying the runaway electron formation processes.

First principle modelling of the runaway electron formation in Ohmic discharges performed in the Tore Supra tokamak is carried out with the 3-D linearized bounce-averaged relativistic Fokker-Planck solver LUKE, using plasma parameters such as parallel electric field and the toroidal MHD equilibrium calculated with the fast integrated modelling tool, METIS. The METIS/LUKE simulations yield the evolution of the electron distribution function and runaway electron population. Details of the fast electron distribution function are presented, as well as quantitative comparison with non-thermal bremsstrahlung emission profiles.

1 Introduction

Runaway electrons can form in tokamak plasmas when the toroidal electric field E exceeds some critical value

$$E_c = \frac{n_e e^3 \ln\Lambda}{4\pi\epsilon_0^2 m_0 c^2}, \tag{1}$$

where n_e is the electron density, m_0 is the electron rest mass, c is the speed of light, e is the elementary charge and $\ln\Lambda$ is the Coulomb logarithm [1].

Runaway electrons may cause serious damage to plasma facing components in ITER [2]. They may appear during plasma disruptions, current ramp-up or ramp-down and even in the current flattop in quiescent low density plasmas as observed in several tokamaks [3, 4, 5].

Processes of runaway electron formation, including runaway avalanches as a result of knock-on collisions between relativistic and thermal electrons, are implemented in the code LUKE, a solver of the 3-D (one spatial and two momentum dimensions) linearized bounce-averaged relativistic electron Fokker-Planck equation in toroidal geometry [6, 7]. The primary runaway electron formation is in good agreement between the LUKE code and the Fokker-Planck solver CQL3D [8], including the effect of magnetic trapping in a non-uniform magnetic field [6]. Other numerical tools for studying runaway electrons include CODE [9], which is a 2-D momentum space code, but has no spatial dependency so that any effect due to radial profile or non-uniformity of the magnetic field is neglected. The Monte Carlo code ARENA [10] has been used to study formation of runaway electrons. LUKE, being a finite difference code, has a fundamentally different approach to solving the time evolution of the bounce-averaged distribution function. The advantage of Monte Carlo codes for runaway electron studies is the ability to follow particles in the presence of complex or stochastic magnetic fields, a domain that is not entered in this work.

The runaway electron formation mechanisms implemented in the LUKE code are benchmarked with analytical expressions in a recent publication [7]. In this work we aim to validate the runaway formation model against experimental observations. With the current status of the tools, we are restricted to scenarios with small runaway electron population, such that the effect of the runaway electron distribution on the electric field is negligible. Quiescent scenarios with non-transient equilibria are therefore most suitable for the validation of the model in its current state. Interpretative kinetic modelling of the runaway formation in the current flattop of scenarios in the Tore Supra (TS) tokamak is performed. Plasma parameters such as parallel electric field and plasma equilibrium are prescribed by the fast integrated modelling code METIS (Minute Embedded Tokamak Integrated Simulator) [11]. Even though runaway electron experiments on the TS tokamak are often dedicated to disruption studies [12], a limited number of well-diagnosed non-disruptive scenarios with runaway electrons are available in the database. Two consecutive low density non-disruptive TS discharges are identified. Runaway electrons are detected in the TS tokamak in low line-averaged density discharges ($\bar{n}_e < 10^{19}\ m^{-3}$) in the current ramp-down by hard X-ray (HXR), photo-neutron and electron cyclotron emission (ECE) measurements [7]. Such signatures are found in discharge #40719, where the line-averaged electron density in the current flattop is $\bar{n}_e = 0.64 \cdot 10^{19} m^{-3}$, corresponding to $E/E_c \approx 8$, or $E/E_D \approx 0.06$, where $E_D = E_c m_0 c^2/T_e$ is the Dreicer field. However, in a similar discharge (#40721), with a two times higher density, no runaway electrons are observed even though the electric field exceeds also the critical electric field ($E/E_c \approx 4$, or $E/E_D \approx 0.02$).

In addition to these discharges being suitable for validation of the LUKE code, it is interesting to relate the results to recent studies of the effective critical electric field, which is found to be several times larger than the critical electric field predicted by collisional theory (Eq. 1) [1]. The two TS discharges studied in Ref. [7] are found to match the experimental threshold electric field ($E \approx (3-5)E_c$) observed across several tokamaks [4, 5]. The elevated threshold electric field could be explained by the effect of electron temperature, that comes into play when starting from a Maxwellian electron distribution function. The primary runaway electron mechanism may be too weak for relevant bulk electron temperatures [7]. In addition synchrotron radiation may damp the runaway electron growth rate [13]. The HXR detectors have finite sensitivity to runaway electrons, and therefore minimum levels of detectable runaway electron populations [4]. Consequently the absence of runaway electron signatures on the detectors does not necessarily guarantee that no runaway or suprathermal electrons are effectively formed. The kinetic modelling of the electron distribution function allows for investigation of the runaway electron dynamics beyond experimental limitations, which may contribute to understanding of runaway electron formation processes.

The modelling chain is described in Sec. 2, along with the results of the TS discharges (#40719 and #40721) in near critical field. In Sec. 3 the simulations are validated by comparison with experiments, in particular with fast electron bremsstrahlung profiles from the HXR tomographic system by reconstruction of the HXR signal from the electron distribution function with the tool R5-X2 [14].

2 Modelling of non-disruptive tokamak discharges

In order to understand the different outcome of the two non-disruptive TS scenarios, the formation of runaway electrons from the combined effect of Dreicer acceleration and knock-on collisions is studied with the LUKE code [7]. The global discharge evolution, MHD equilibrium and kinetic profiles for each plasma scenario are obtained from the fast integrated tokamak simulator METIS, which solves the current diffusion equation assuming an approximate equilibrium evolution [11]. The METIS code provides interpretative simulations of Tore Supra discharges yielding particle and impurity densities, ion and electron temperature profiles, bootstrap current and plasma momentum. The electric field radial profile parallel to the magnetic field lines $E_{\|}(r,t)$, used for simulation of inductive discharges is also calculated with METIS. Temperature and density profiles are prescribed in METIS by fitting the combined results of a set of diagnostics including Thomson scattering, ECE, reflectometry and interferometry, weighted with Bayesian analysis [15].

Given the METIS toroidal MHD equilibria, the effect on the electron distribution function is calculated with the LUKE code [7]. Its time evolution is considered and the external runaway electron population n_{re} (with kinetic energy $E_k > 1$ MeV) at the end of each time slice (index $t-1$) is used as input for the following time step (t):

$$n_{re,init,t} = n_{re,end,t-1}, \tag{2}$$

which is equivalent to assuming that the runaway electrons remain confined throughout the entire discharge at the flux surface coordinate where they were formed. The '*init*' index denotes that the value or function is used as initial value in the time slice. Given this criteria, the time slice has to be small for the equilibrium to remain rather constant within the time slice.

The momentum grid of the LUKE code is normalized to the local thermal momentum. As a consequence the grid needs to be normalized according to the temperature changes and input from previous time steps are interpolated onto the new momentum grid. In the first time step the initial distribution function is taken to be Maxwellian (f_M). Given the initial distribution function the effect on the distribution function during the time dt_n is calculated with the LUKE code. The internal runaway electron population, i.e the electrons with $E_k < 1$ MeV but above the force balance boundary, is transferred between time steps by interpolating the electron distribution function onto the new momentum grid. The calculated distribution function is used as initial distribution function in the consecutive time step, with local temperature and density ($n_b = n_e - n_{re}$) updated through addition/subtraction of a Maxwellian function and by a normalization onto the momentum grid, itself normalized to the new thermal momentum. Thus, the evolution of the distribution function becomes

$$\begin{aligned} f_{init,0} &= f_M(n_{e0}, T_{e0}), && (3) \\ f_{init,t} &= f_{end,t-1} + (n_{b,t} - n_{b,t-1}) f_M(n_{e,t}, T_{e,t}). && (4) \end{aligned}$$

2.1 Runaway discharge #40719

Line-averaged electron density, plasma current and parallel electric field strength in discharge #40719 are presented in Fig. 1a. The central electric field evolution as calculated by METIS normalized to E_c is shown in Fig. 1b.

For #40719 the METIS/LUKE simulations show that runaway electrons are progressively formed during the current flattop (Fig. 2a), concentrated near the magnetic axis. Even though the density is lower off-axis than in the core and the E-field profile is rather flat, E/E_D decreases with the radius due to the low temperature at the plasma edge. This could explain the slower Dreicer generation off the magnetic axis. Also, the increase of magnetic trapping effects contributes to a reduced runaway growth rate off-axis as the overall effect of the electric field on trapped electrons cancels out over one bounce period [7]. The reduction of the runaway electron growth rate has recently been quantified through bounce-averaged calculations in Ref. [7].

Figure 2b shows the calculated current density profile as carried by runaway electrons with kinetic energy $E_k > 1$ MeV, when assuming that they move at the speed of light. The current density carried by runaway electrons is very centrally concentrated as compared to the bulk current. The METIS/LUKE calculated

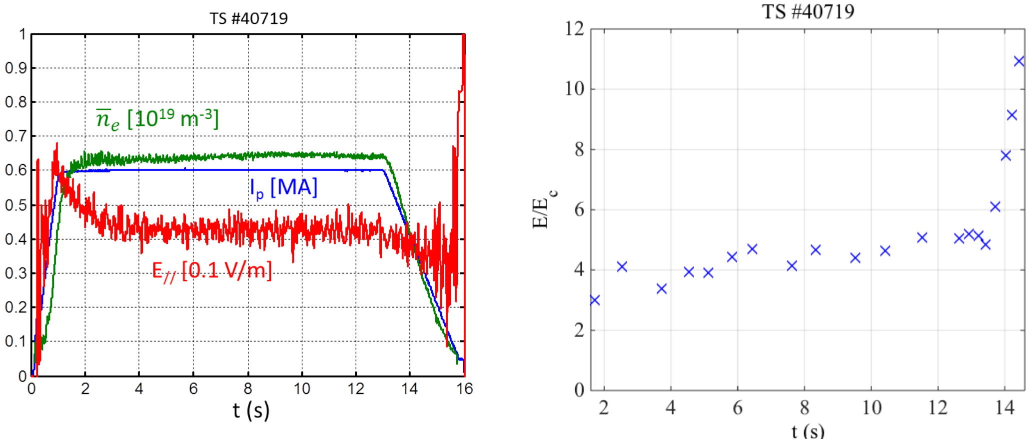

(a) (b)

Figure 1: Line-averaged electron density, plasma current and parallel electric field strength in discharge #40719 (a). The central electric field evolution as calculated by METIS in discharge #40719 (b).

Ohmic plasma current during the current flattop is 0.54 MA, compared to the experimental plasma current of 0.55 MA. METIS provides a 0-D effective charge value based on bremsstrahlung, temperature and density measurements and thus a flat profile is used as input for LUKE. To match the plasma currents, the effective charge has been reduced from the one used in METIS, $Z_{eff} = 3.9$ to $Z_{eff} = 2.9$. Simulations are performed only until around 14.5 s, as the density and temperature profile measurements become uncertain from this point. The reduced Z_{eff} value required to match the plasma current may be an indication of that the effective charge is lower centrally than towards the edge, as the METIS prediction of Z_{eff} is principally representative of the value near the edge. One explanation for a radial dependence could be screening near the center by inward flux of carbon from the wall that reduces Z_{eff} in the center, which is typical for a flat density and peaked temperature profile.

In the calculations bounce-averaging is necessary to correctly describe the 2-D momentum electron dynamics in the non-uniform magnetic field. To quantify the effect of the bounce-average we compare the runaway electron population of the fully bounce-averaged calculation with simulations where the bounce-average is switched off for the discharge #40719. Near the magnetic axis the non-bounce-averaged calculation coincides with the bounce-averaged solution, as expected due to the absence of magnetic trapping effects on the magnetic axis. However, as seen in Fig. 3 the bounce averaging reduces the runaway electron population significantly off the magnetic axis. At $\rho \geq 0.25$ the number of runaway electrons is less than 20% as compared to central values. In the non-bounce-averaged calculations the runaway electron profile is broader, but still

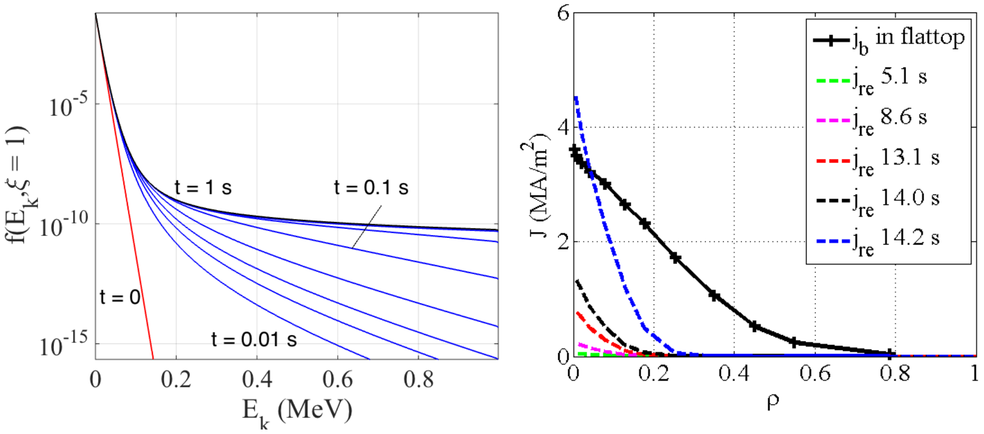

(a) Electron distribution function at $\xi = 1$ in current flattop during 1 s.

(b) Current density of bulk (black) and current density carried by runaway electrons ($E_k > 1\,\mathrm{MeV}$).

Figure 2: Modelling results from TS discharge #40719.

centrally concentrated as a consequence of the temperature profile, and reduced E/E_D off-axis.

An additional signature of the existence of runaway electron population is the remaining plasma current ($\sim 50\,\mathrm{kA}$) at $15.7-16$ seconds, during the termination of the plasma as seen in Fig. 4. This remaining current plateau is believed to originate from a beam of well confined runaway electrons, as discussed in Ref. [7]. Such a current is not observed in the higher density discharge (#40721). At the end of the current flattop the METIS/LUKE predicts that the current carried by external runaway electrons ($E_k > 1\,\mathrm{MeV}$) is 20 kA, which is consistent with observations at the end of the ramp-down ($I_p = 50\,\mathrm{kA}$).

However, during the current ramp down LUKE predicts that the current carried by runaway electrons increases dramatically. The explanation results from the electric field profiles predicted by METIS. During the current flattop, the electric field profile is flat. Due to current diffusion, the decrease of the electric field starts at the edge in these discharges. With time the electric field drops also towards the magnetic axis. However, very close to the magnetic axis ($\rho < 0.2$) the electric field remains at the same level during the entire ramp down as during the current flattop despite a significant fraction of runaway electrons that would locally give rise to a high plasma current density that should reduce the local electric field strength. In this current ramp-down there is therefore a need for self-consistent calculations of the electric field with the runaway electron current, as E/E_c and E/E_D increases significantly and the current carried by runaway electrons becomes significant. This can be seen also in Fig. 4, where in the current ramp-down (t>13 s) the current carried by runaway electrons becomes comparable to the Ohmic current in the center.

Another explanation to the overestimated runaway electron population could

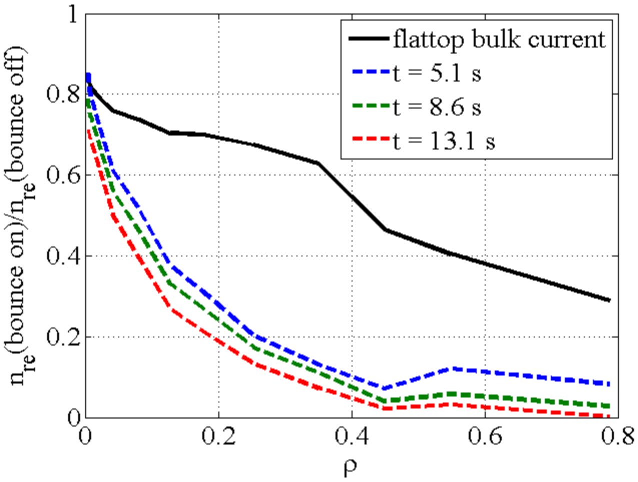

Figure 3: Population of runaway electrons with kinetic energy $E_k > 1$ MeV given by the full bounce-averaged calculation, normalized to the calculation for which the bounce-averaging is turned off. The solid black line shows the bounce-averaged current density profile normalized to the bulk current density without bounce-average.

be that in the model loss mechanisms of fast electrons are neglected. In reality runaway electrons are not well confined, but they escape the plasma throughout the current flattop, and especially during the current (and density) ramp-down [4].

2.2 Non-runaway discharge #40721

With METIS/LUKE simulations we can investigate whether any suprathermal electrons are formed in a discharge without runaway signature like discharge #40721, where $E > E_c$. The simulation of discharge #40721 confirms the experimental observations; the population of suprathermal electrons is negligible and the electron distribution function hardly deviates from the initial Maxwellian distribution function through the discharge, see Fig. 5. The external runaway population, i.e. electrons with kinetic energy $E_k > 1\,\mathrm{MeV}$, is so small that it would only carry a negligible current at the end of the 10 seconds long current flattop (∼mA).

The results are consistent with the parametric study of runaway formation performed in Ref. [7], where it is found that forming a significant runaway electron population from an initial Maxwellian distribution in a 3 keV plasma in the local central electric field strength $E/E_c \approx 2.5$, requires longer duration than the 10 second duration of the flattop. Furthermore, these results support the experimental observations of Ref. [4] where at least $E/E_c \sim 3-12$ is required

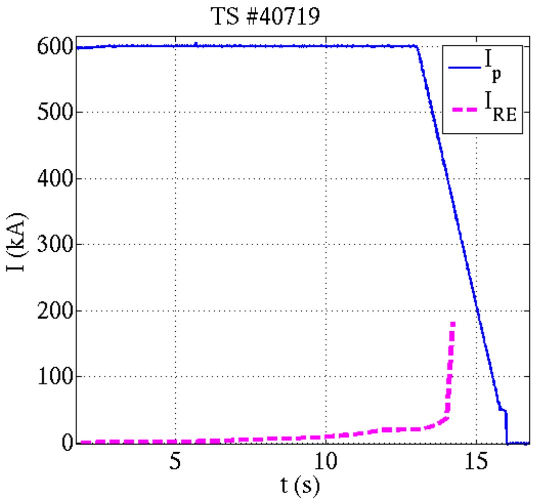

Figure 4: Current carried by runaway electrons (I_{RE}), as calculated by METIS/LUKE, compared to the plasma current (I_p).

to generate a detectable population of runaway electrons in various tokamaks. Thus, the critical electric field E_c is not a sharp criterion for runaway electron formation.

3 Fast electron bremsstrahlung reconstruction

In order to validate the METIS/LUKE modelling results for the runaway electron discharge the simulations are compared to experimental measurements through reconstructed HXR tomography emission based on the electron distribution function with the R5-X2 code [14]. Given an electron distribution function calculated by LUKE, it predicts the fast electron bremsstrahlung (FEB) cross-section and integrates the emission along the lines of sight, accounting for the response function of the detectors. The HXR signals from a vertical (chords $1-21$) and horizontal (chords $22-59$) cameras provide information about the suprathermal electron population.

During discharge #40719 the signal of the horizontal central chord (#41) is found to be at least the double amplitude of the central chord of the vertical camera (#14), until around 12 s into the discharge where the signals are within 25% of each other. Therefore we restrict the analysis of the HXR tomographic signals to the end of the current flattop (t>12 s).

The HXR reconstruction with R5-X2 in the energy range $50-110\,\mathrm{keV}$ is compared with the experimental count rate profile in Fig. 6. The FEB emission profile reconstruction based on LUKE simulations predicts a runaway electron population concentrated near the magnetic axis, as seen in Fig. 7, corresponding to a beam of diameter around 25 cm The shape and amplitude of reconstructed

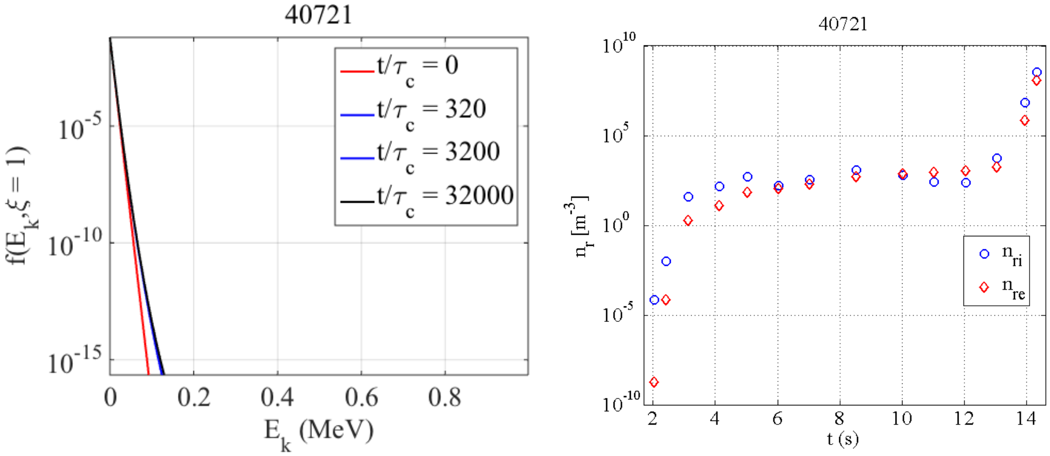

(a) Electron distribution function at $\xi = 1$ in current flattop during 1 s.

(b) Internal (n_{ri}) and external (n_{re}) runaway electron population.

Figure 5: Modelling results from TS discharge #40721 show that the formation of runaway electrons is negligible.

FEB emission show reasonable agreement with measurements.

In addition to bremsstrahlung from suprathermal electrons the HXR detectors are sensitive to fusion neutrons as well as interaction between the plasma and the wall. The vertical and horizontal cameras view the poloidal cross-section of the plasma, which in the case of these Tore Supra discharges is circular. Therefore, signals from suprathermal electrons in the plasma should be of comparable amplitude, to be free from any artificial signal from background noise. An offset in the HXR signal is observed on the horizontal camera (chords 22-59). Similar observation has previously been seen on FEB emission profiles from Tore Supra in Ref. [16], where localized populations of suprathermal electrons lead to back scattered x-rays off the high field side inner wall. Chord #11 on the vertical camera corresponds to the last closed flux surface (LCFS) is tangential to the toroidal limiter. The elevated peak on chord #11 in Fig. 6 may indicate a radial transport of fast electrons, i.e. thick target bremsstrahlung emission due to plasma-limiter interaction.

The measured count rate signal for discharge #40721 is around noise level, i.e. $0 - 4\ s^{-1}$ in each chord. The METIS/LUKE simulations predict, in agreement, a negligible count rate signal ($0 - 1\ s^{-1}$).

4 Conclusion

In previous work (Ref. [7]), the model for runaway electron formation is benchmarked with analytical expressions. In this work, the first interpretative modelling is performed for real Tore Supra non-disruptive discharges with detected

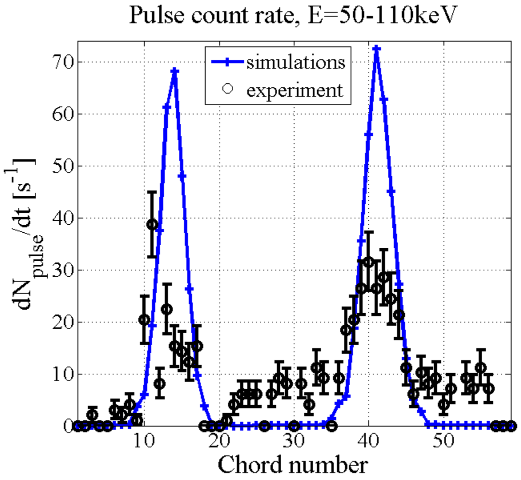

Figure 6: Reconstructed FEB profile from the LUKE calculated electron distribution function, compared to measured FEB emission from HXR cameras for discharge #40719.

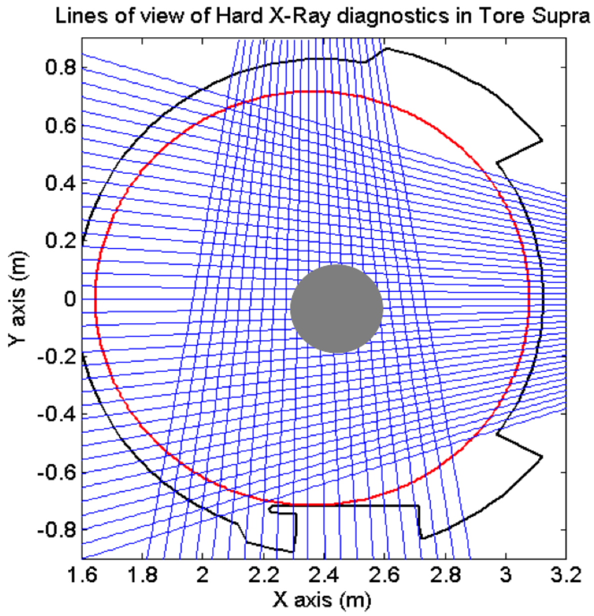

Figure 7: The location of the suprathermal electrons, as predicted by the LUKE calculations, corresponds to a beam of diameter ~ 25 cm.

runaway electrons. The Fokker-Planck solver LUKE, is used to model runaway electron formation through Dreicer and avalanche mechanisms in non-disruptive Tore Supra scenarios in near-critical E-field with the background plasma simulated with the METIS code. Simulations reveal progressive build-up of a suprathermal population during the flattop in the discharge where runaway electrons are detected (#40719), but not in the higher density discharge (#40721) where $E/E_c \approx 2.5$ locally. These results agree with experimental observations from various other tokamaks [4] where $E/E_c \approx 3-12$ is required for a detectable runaway population to form. The order of magnitude of the current carried by runaway electrons agrees with experimental indications at the end of the current flattop. The magnitude of the reconstructed FEB emission from suprathermal electrons is well reproduced and shows concentration of runaway electrons in the center of the plasma. Even though the density is lower off-axis, the temperature profile makes E/E_D decrease with the radius which would explain the slower Dreicer generation. Also, as discussed in Ref. [7], magnetic trapping effects increase off-axis, adding further to the slower Dreicer generation rate.

Non-disruptive scenarios are well suitable for validation of the modelling codes, as such scenarios are better diagnosed and initial conditions and equilibrium are well defined as compared to disruptive scenarios. In the type of discharges presented in this work, the runaway population is small and the current carried by runaway electrons has a negligible effect on the parallel E-field. However, in scenarios where the runaway current is more than just a perturbation of the Ohmic current, the toroidal electric field would need to be calculated self-consistently with the runaway electron population. In the ramp down of discharge #40719 there appears to be a need for self-consistent calculations as the calculated runaway electron population grows faster than what is seen in experiments. The central electric field must decrease in the presence of a local significant runaway electron population. The METIS simulations are performed without accounting for the presence of runaway electrons, an assumption that is valid during the current flattop of discharge #40719. As soon as the runaway population becomes significant, in this case in the current ramp down, the electric field strength and thus the following evolution of the runaway electron population gets overestimated. In order to make reliable predictions also for scenarios with a strong runaway electron formation a self-consistent coupling between the electric field in METIS and the runaway electron population in LUKE is foreseen as the next step in this work.

Acknowledgement This work has been carried out within the framework of the EUROfusion Consortium and has received funding from the Euratom research and training programme 2014-2018 under grant agreement No 633053. The views and opinions expressed herein do not necessarily reflect those of the European Commission.

References

[1] H. Dreicer. Electron and ion runaway in a fully ionized gas. i. *Phys. Rev.*, 115(2):238–249, 1959.

[2] T. C. Hender, J.C Wesley, J. Bialek, A. Bondeson, A.H. Boozer, R.J. Buttery, A. Garofalo, T.P Goodman, R.S. Granetz, Y. Gribov, O. Gruber, M. Gryaznevich, G. Giruzzi, S. Günter, N. Hayashi, P. Helander, C.C. Hegna, D.F. Howell, D.A. Humphreys, G.T.A. Huysmans, A.W. Hyatt, A. Isayama, S.C. Jardin, Y. Kawano, A. Kellman, C. Kessel, H.R. Koslowski, R.J. La Haye, E. Lazzaro, Y.Q. Liu, V. Lukash, J. Manickam, S. Medvedev, V. Mertens, S.V. Mirnov, Y. Nakamura, G. Navratil, M. Okabayashi, T. Ozeki, R. Paccagnella, G. Pautasso, F. Porcelli, V.D. Pustovitov, V. Riccardo, M. Sato, O. Sauter, M.J. Schaffer, M. Shimada, P. Sonato, E.J. Strait, M. Sugihara, M. Takechi, A.D. Turnbull, E. Westerhof, D.G. Whyte, R. Yoshino, H. Zohm, the ITPA MHD, Disruption, and Magnetic Control Topical Group. MHD stability, operational limits and disruptions. *Nucl. Fusion*, 47:S128–S202, 2007.

[3] R. Jaspers, K.H. Finken, G. Mank, F. Hoenen, J.A. Boedo, N.J.L. Cardozo, and F.C. Schuller. Experimental investigation of runaway electron generation in TEXTOR. *Nuclear Fusion*, 33(12):1775, 1993.

[4] R. S. Granetz, B. Esposito, J. H. Kim, R. Koslowski, M. Lehnen, J. R. Martin-Solis, C. Paz-Soldan, T. Rhee, J. C. Wesley, and L. Zeng. An ITPA joint experiment to study runaway electron generation and suppression. *Physics of Plasmas*, 2014.

[5] C. Paz-Soldan, N. W. Eidietis, R. Granetz, E. M. Hollmann, R. A. Moyer, J. C. Wesley, J. Zhang, M. E. Austin, N. A. Crocker, A. Wingen, and Y. Zhu. Growth and decay of runaway electrons above the critical electric field under quiescent condition. *Physics of Plasmas*, 21, 2014.

[6] J. Decker and Y. Peysson. DKE: A fast numerical solver for the 3D drift kinetic equation. report EUR-CEA-FC-1736, Euratom-CEA, 2004.

[7] E. Nilsson, J. Decker, Y. Peysson, R.S Granetz, F. Saint-Laurent, and M. Vlainic. Kinetic modelling of runaway electron avalanches in tokamak plasmas. *Plasma Phys. and Controlled Fusion*, 57(9):095006, 2015.

[8] R.W. Harvey and M.G. McCoy. The CQL3D Fokker-Planck code. In *IAEA Technical Committee on Advances in Simulation and Modeling of Thermonuclear Plasmas*, pages 489–526, 1992.

[9] M. Landreman, A. Stahl, and T. Fülöp. Numerical calculation of the runaway electron distribution function and associated synchrotron emission. *Computer Physics Communications*, 185(3):847 – 855, 2014.

[10] L. G. Eriksson and P. Helander. Simulation of runaway electrons during tokamak disruptions. *Comp. Phys. Comm.*, 154:175–196, 2003.

[11] J. F. Artaud, V. Basiuk, F. Imbeaux, M. Schneider, J. Garcia, G. Giruzzi, P. Huynh, T. Aniel, F. Albajar, J. M. Ane, A. Bécoulet, C. Bourdelle, A. Casati, L. Colas, J. Decker, R. Dumont, L.G. Eriksson, X. Garbet, R. Guirlet, P. Hertout, G. T. Hoang, W. Houlberg, G. Huysmans, E. Joffrin, S.H. Kim, F. Köchl, J. Lister, X. Litaudon, P. Maget, R. Masset, B. Pégourié, Y. Peysson, P. Thomas, E. Tsitrone, and F. Turco. The CRONOS suite of codes for integrated tokamak modelling. *Nucl. Fusion*, 50(4):043001, 2010.

[12] F. Saint-Laurent, G. Martin, T. Alarcon, A. Le Luyer, P. B. Parks, P. Pastor, S. Putvinski, C. Reux, J. Bucalossi, S. Bremond, and Ph. Moreau. Overview of runaway electron control and mitigation experiments on Tore Supra and lessons learned in view of ITER. *Fusion Science and Technology*, 64(4):711–718, 2013.

[13] A. Stahl, E. Hirvijoki, J. Decker, O. Embreus, and T. Fülöp. Effective critical electric field for runaway-electron generation. *Phys. Rev. Letters*, (114):115002, 2015.

[14] Y. Peysson and J. Decker. Fast electron bremsstrahlung in axisymmetric magnetic configuration. *Phys. Plasmas*, 15(9):092509, 2008.

[15] M. Irishkin. *Comparaison automatisée de reconstructions Bayésiennes de profils expérimentaux avec des modèles physiques.* PhD thesis, Aix Marseille Université, 2014.

[16] Y. Peysson, P. Froissard, and C. Pocheau. Study of radiation scattering in the hard X-ray energy range by a tokamak inner wall. *Nucl. Fusion*, 33(8):1133–1145, 1993.